

Critical evaluation of the thermal performance analysis of a new cooling tower prototype

P. Navarro ^a, J. Ruiz ^{b,*}, M. Hernández ^a, A.S. Kaiser ^a, M. Lucas ^b

^a Departamento de Ingeniería Térmica y de Fluidos, Universidad Politécnica de Cartagena, Dr. Fleming, s/n, 30202 Cartagena, Spain

^b Departamento de Ingeniería Mecánica y Energía, Universidad Miguel Hernández, Avda. de la Universidad, s/n, 03202 Elche, Spain

ARTICLE INFO

Keywords:

Cooling tower
Thermal performance
Flow arrangement
Merkel
Poppe

ABSTRACT

This paper presents a critical evaluation of the thermal performance analysis of the inverted cooling tower, which was conceived as a new cooling tower prototype that prevents the dispersion of pollutants to the atmosphere during its operation. The device can be classified as a mechanical forced draft, counterflow-parallel flow cooling tower.

The combination of the Merkel and Poppe methods of analysis and the counterflow, parallel and counterflow/parallel flow arrangements has been discussed, for a total of 5 different approaches. The Poppe method for thermal performance prediction reports higher Merkel numbers than the Merkel method: from 3.84% to 6.64%. A higher Merkel number is obtained for the parallel arrangement compared to counterflow to achieve the same cooling. Differences from 1.12% to 12.19% are observed for the range of tested water-to-air mass flow ratios.

The rigorous method that uses the Poppe theory and combines counterflow and parallel flow arrangements (main novelty of this paper) is recommended to evaluate the thermal performance. Not only it provides the best predictions for the outlet water and air temperatures (0.44 °C difference for the water prediction and 0.74 °C difference for the air) but it is a good approximation of the complex underlying physics of the problem and the state of the outlet air is accurately determined.

1. Introduction

Cooling towers are heat rejection systems used to dispose of unwanted heat from power plants, refrigeration cycles and industrial processes. In a cooling tower, waste heat is transferred from the cooling water to the atmospheric air stream by convection and, mainly, evaporation of water.

Unsaturated moist air entering the tower exchanges heat and mass due to temperature and concentration differences between water and air streams. Part of the water evaporates while the rest cools down. The heat is rejected to the atmosphere as warm moist air.

Cooling towers can create aerosols (droplets of water in the air) during their operation because some part of the water that have not evaporated can be taken away by the air stream to the atmosphere. This phenomenon is usually regarded as drift and it has been reported by several authors as an environmental and a health hazard [1–5].

Concerning human health, the spreading of the legionella bacteria is the main concern. If legionella contaminated water droplets are sent into the air and carried by the wind, they can then be inhaled by those people present in the affected area of the tower and cause several lung conditions of varying severity such as Legionnaires' disease.

In order to minimise the cooling tower environmental impact, a novel cooling tower prototype was analysed in Ruiz et al. [6]. The inverted cooling tower, as termed by the authors, was conceived as a new cooling tower design that prevents the dispersion of water droplets to the atmosphere during its operation (Fig. 1).

The inverted cooling tower presents two main differences with conventional cooling towers. The first one is the location of the inlet and outlet areas. The air intake takes place at the top of the tower while it is discharged at the bottom. The second difference concerns the water and air flow arrangements. In the novel design, water flows upwards from the nozzles to the fan until the inertia and drag forces balance, and then downwards to and through the fill, to finally be collected in the tower basin, Fig. 2. In a singular way, it can be classified as a mechanical forced draft, counterflow-parallel flow, wet cooling tower.

The authors assessed, through experimental calculation, that the performance of the tower in terms of emissions was remarkably low. Drift emissions were found to be up to 300 times lower than the limits imposed by several international standards: 0.00015% of the circulating water compared to 0.05% (Royal Decree RD 865/2003 [7] in

* Corresponding author.

E-mail address: j.ruiz@umh.es (J. Ruiz).

Nomenclature

A	frontal area (m^2)
a_V	surface area of exchange per unit of volume ($m^2 m^{-3}$)
c_p	specific heat ($J kg^{-1} K^{-1}$)
f	frequency level of the fan (Hz)
h	enthalpy ($J kg^{-1}$)
h_C	heat transfer coefficient ($W m^{-2} K^{-1}$)
h_D	mass transfer coefficient ($kg m^{-2} s^{-1}$)
j	Coefficient in the Runge–Kutta method
k	Coefficient in the Runge–Kutta method
l	Coefficient in the Runge–Kutta method
Le	Lewis number ($= h_C / (h_D c_{p,ma})$)
\dot{m}	mass flow rate ($kg s^{-1}$)
Me	Merkel number ($= h_D a_V V / \dot{m}_w$)
N	Number of intervals considered in the Runge–Kutta method
n	Number of levels considered in the Runge–Kutta method
\dot{Q}	total heat transferred from water to air (W)
\dot{Q}_s	sensible heat transferred from water to air (W)
\dot{Q}_l	latent heat transferred from water to air (W)
T	temperature (K)
V	volume of the transfer region (m^3)
z	height (m)

Greek symbols

ρ	density ($kg m^{-3}$)
ω	humidity ratio ($kg kg^{-1}$)

Subscripts

a	air
i	intermediate
ma	moist air
M	Merkel
P	Poppe
s	saturated
v	vapour
w	water
1	inlet
2	outlet

Spain) and 0.02% (Australian Standard AS/NZS 3666 [8] in Australia), respectively. This value represents a reduction ranging from 40.21% to 82.54% compared to commercial towers. Nonetheless, despite the high potential reduction in the emission level, the observed thermal performance results were more modest. The efficiency of the tower was similar to that of a commercial tower equipped with a film-flow distribution system (up to 6.98% better). The difference is larger (41.16% lower) when compared to the same tower equipped with a splash distribution system.

It should be noted that in this study, the authors used the Merkel theory for thermal performance prediction and cooling was assumed to occur only in countercurrent arrangement. This fact constituted a critical assumption concerning the thermal performance calculation since in the inverted cooling tower, the cooling takes place in two different flow arrangements: counterflow and parallel.

The influence of the flow arrangement and the Merkel and Poppe methods for thermal performance prediction on the performance of



Fig. 1. Built prototype of the inverted cooling tower.

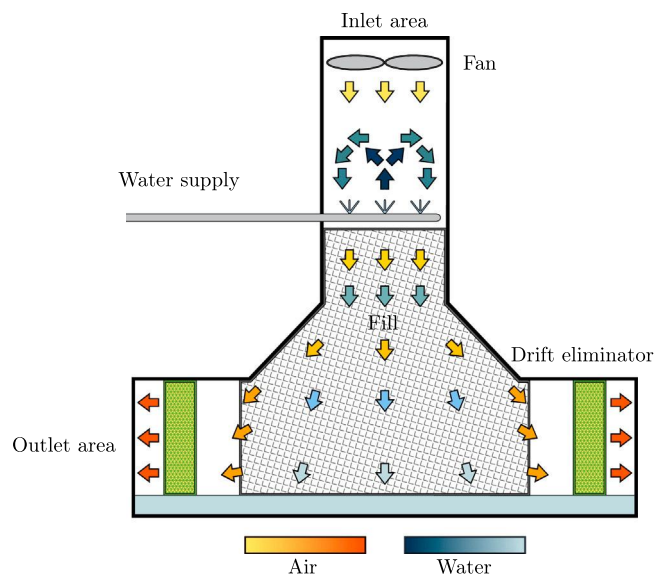


Fig. 2. Schematic of the new prototype of wet cooling tower highlighting the counterflow-parallel flow arrangements and the main parts of the tower.

the inverted cooling tower was addressed by Ruiz et al. [9]. The authors pointed out that, for a rigorous characterisation of the thermal performance of the tower, it was necessary to know the amount of cooling taking place in each flow arrangement. This fact constituted the main motivation of this work.

The analysis of wet cooling towers through modelling has its origin a century ago, in the 1920s. Merkel [10] developed the theory for the performance evaluation of cooling towers. The author proposed a model based on several critical assumptions to reduce the solution of heat and mass transfer in wet-cooling towers to a simple hand calculation. Because of these assumptions, however, the Merkel method does not accurately represent the physics of the heat and mass transfer process in the cooling tower. Bourillot [11] stated that the Merkel method is simple to use and can correctly predict cold water temperature when an appropriate value of the coefficient of evaporation is used. In contrast, it is insufficient for the estimation of the characteristics of the warm air leaving the fill and for the calculation of changes in the water flow rate due to evaporation. These quantities are important to estimate water consumption and to predict the behaviour of plumes exiting the cooling tower. Jaber and Webb [12] developed the equations

necessary to apply the effectiveness-NTU method directly to counterflow or crossflow cooling towers. This approach is particularly useful in the latter case and simplifies the method of solution when compared to a more conventional numerical procedure. The effectiveness-NTU method is based on the same simplifying assumptions as the Merkel method. Poppe and Rögner [13] developed the Poppe method. They derived the governing equations for heat and mass transfer in a wet cooling tower and did not make any simplifying assumptions as in the Merkel theory. Predictions from the Poppe formulation result in values of evaporated water flow rate that are in good agreement with full scale cooling tower test results. In addition, the Poppe method predicts the water content of the exiting air accurately.

Several studies can be found in the literature using the Merkel, effectiveness-NTU and Poppe methods for thermal performance evaluation of evaporative devices for different purposes.

Performance analysis is a common application for using the Merkel and Poppe theories. Concerning the Merkel method, Ke et al. [14] numerically and experimentally analysed the heat and mass transfer on air/water direct contact in a humidifier. They also made a comparison with the Poppe method, which they used in previous calculations and concluded that with the Merkel theory the numerical results were closer to the experimental results. In Mishra et al. [15] a silica gel mesh (SGM) column was installed at the inlet of the cooling tower and the performance of the system was investigated. Zengin and Onat [16] studied the pressure losses and the thermal performance in a cooling tower with different cooling fill heights. In Ruiz et al. [6], the thermal performance analysis of the inverted cooling tower was carried out. Other studies use the Poppe theory to address also the performance analysis. Huang et al. [17] analysed the performance of a novel evaporation system based on a humidification–dehumidification process. Zhou et al. [18] investigated the thermal performance of a new Closed Wet Cooling Tower (CWCT). Bamimore et al. [19] investigated the effect of certain parameters on the performance of an industrial cooling tower. Tomas et al. [20] analysed the performance of new alternative materials as filling for cooling towers.

Performance optimisation is another common use of Poppe and Merkel methods. In Keshtkar [21], the Poppe method was used to investigate the optimum operative conditions of a specific cooling tower. The obtained results were compared to the results obtained using the TOPSIS method. Huang et al. [17] and Li et al. [22] used the Poppe method to optimise the operation of a humidification–dehumidification evaporation system. In Singh and Das [23], the Merkel method was used to perform a simultaneous optimisation of performance parameters and energy consumption in induced draft cooling towers. Liao et al. [24] compared the Merkel, Braun, and Halasz models with the objective of applying them to optimise the cooling tower approach temperature control schedule in a cooling system.

Another method used by some authors is the effectiveness–NTU. Sharqawy et al. [25] used this method to analyse the thermal performance of packed-bed cross-flow humidifier. Ayoub et al. [26] presented a model of a natural draft wet type cooling tower, which is based on the conservation laws of thermodynamics and compared the results obtained with the Poppe, Merkel and effectiveness–NTU methods.

A detailed comparison between methods for thermal performance prediction can be found in Kloppers [27] and Kloppers and Kröger [28]. The authors concluded that the Merkel number according to the Poppe method is greater than the Merkel number predicted by the Merkel method. The Poppe method provides a more accurate representation of the physics of the problem (predicts the evolution of the moist air and allows to calculate the evaporated water). Thus, the Poppe method is recommended in the analysis of cooling towers where the state of the outlet air needs to be accurately determined. The Merkel and effectiveness-NTU methods of analysis give approximately identical results as they are based on the same simplifying assumptions.

Given the previous background, the main goal of this paper was to conduct a critical evaluation of the performance characteristics prediction (Merkel number) of the inverted cooling tower. The influence of

the method of analysis (Merkel and Poppe) and the flow arrangement between the water and air streams (counterflow, parallel and counterflow/parallel) on the performance of the tower for a given operating conditions has been discussed. The main novelty is the use of the Poppe model combining two different flow arrangements: parallel and counterflow. Besides, the adaptation of the Poppe model for parallel flow is not an approach commonly found in the literature.

This paper is organised as follows: Section 2 contains the description of the experimental setup, the mathematical modelling, and the experimental procedure for the thermal performance tests. Next, the results obtained in the tests are presented and discussed in Section 3. Finally, the most important findings of the research are summarised in Section 4.

2. Methodology

2.1. Test facility

The experimental tests discussed in this work were carried out in the installation presented in this section. The forced, mechanical-draft, wet cooling tower prototype is located on the roof of the ELDI building, at the Technical University of Cartagena (Spain), Fig. 1. It should be noted that the facility corresponds to the one described in Ruiz et al. [6] with two exceptions. Firstly, two open channels were added at two different heights of the tower to measure the water temperature at additional locations (intermediate water temperature, T_{wi} , onwards). Secondly, the AX model hollow-cone spray nozzles originally installed in the tower were replaced by LAP-PP40 nozzles (both nozzles were manufactured by Spraying Systems Co. Ltd.). The main components installed in the tower and their specifications can be found in Table 1.

The fan drives the air through the interior of the tower, until it reaches the outlet section, which is at ground level and is composed of 4 rectangular-shaped ($3.5 \times 0.7 \text{ m}^2$) faces. The tower has a total height of 3.5 m. The water is driven by a centrifugal pump through the hydraulic circuit, which is formed by a network of polypropylene pipes. Its function is that the water moves from the basin to nine hollow-cone spray nozzles, which are located 1.2 m below the fan in a horizontal position. In this process, the water passes through the boiler, where the thermal load to be dissipated is simulated. Once sprayed, the water is collected in the tower basin after flowing through the trickle-type fill located between the nozzles and the basin.

The experimental thermal performance characterisation of the tower requires to modify the water-to-air mass flow ratio value. This was achieved with two variable frequency drives connected to the fan and pump, respectively. The thermal characterisation also requires the measurement of some key variables: water and air conditions and ambient variables. The sensors installed for this purpose are shown in Fig. 3.

Air measurements include the inlet temperature and relative humidity, and the air velocity. These magnitudes were measured at the inlet and outlet sections of the cooling tower. Eight hot wire anemometers were placed in the centre of each of the faces of the inlet–outlet sections. The ambient temperature and relative humidity were measured by four thermo-hygrometers in the outlet sections and one in the inlet section. With the measurement of the average air velocity at the inlet section, the inlet air specific volume, and the inlet section, the air mass flow rate was calculated.

For the water measurements, the flow rate was measured using an electromagnetic flowmeter while the temperatures were registered at 4 points: before reaching the nozzles, at two different heights inside the tower (to measure the temperature in the highest height reached by the water) and in the discharge of the tower basin. Two open channels were placed at different heights to ensure that the measurement obtained corresponds to the above mentioned temperature (Fig. 3).

Finally, environmental conditions (wind speed and direction, ambient temperature and ambient relative air humidity) were measured,

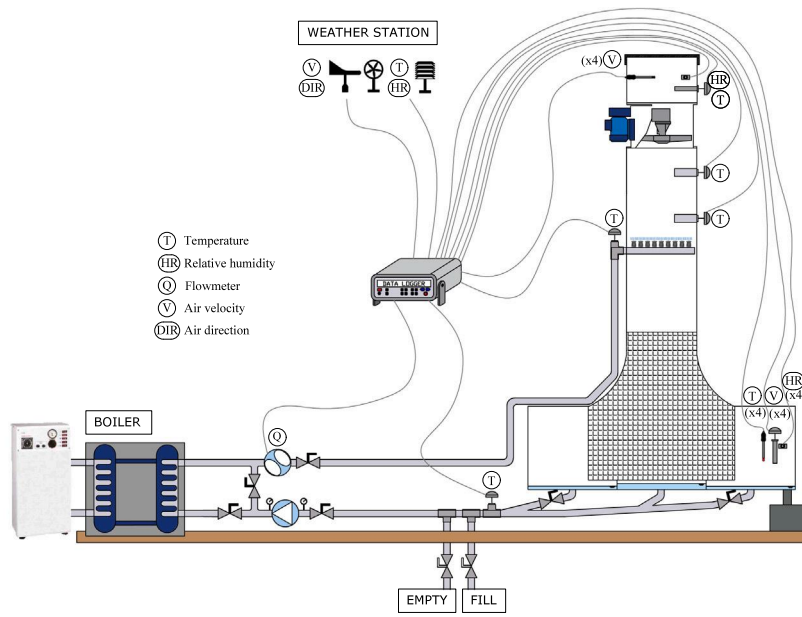


Fig. 3. Schematic of the novel mechanical forced draft wet cooling tower.

Table 1
Component specifications.

Device	Brand	Model	Power (kW)	Technical specifications
Fan	Sodeca	HPX-63-4T-2	1.5	Maximum flow-17500 m ³ h ⁻¹
Pump	Pentax	CBT400	3	5 m ³ h ⁻¹ -6 bar
Nozzles	Spraying Systems	3/8LAP-PP40-40	-	0.492 m ³ h ⁻¹ -0.2 bar
Fill	Control y ventilación	RF240-30	-	Compactness - 200 m ² m ⁻³
Boiler	Gabarrón	CPE45	45	36120 kcal h ⁻¹

Table 2
Sensor devices specifications.

Measurement	Measuring device	Brand	Model	Range	Accuracy	N°
Air velocity	Hot wire anemometer	Distech	PDCSY-AV-622	0-32 m s ⁻¹	±3%	8
Air temperature	Thermohygrometer	Siemens	QFM3160	-40-70 °C	±0.6°C	5
Air humidity				0-100%	±2%	
Water flow rate	Electromagnetic flowmeter	Krohne	OPTIFLUX 1000	-12-12 m ³ s ⁻¹	±0.5%	1
Water temperature	RTD-Pt1000	Siemens	QAE2164.010	-10-120 °C	±0.1%	4

by a meteorological station (Davis Vantage Pro2) located next to the experimental facility, on the roof of the laboratory.

The data from all these sensors was recorded by a ECLYPSE control unit (Distech). Table 2 shows their main specifications: brand, model, measuring range, accuracy and number of sensors installed. This is important information because it will be used in Section 3 to calculate experimental uncertainty values for the water-to-air mass flow ratio and the Merkel number.

2.2. Mathematical modelling

The governing equations for heat and mass transfer in the transfer region of the cooling tower are presented in this section.

2.2.1. Poppe theory for thermal performance evaluation of wet cooling towers

Fig. 4 shows a control volume in the transfer area of a wet cooling tower, where the flow is considered as a one dimensional problem. The figure includes both, the counterflow (Fig. 4(a)) and the parallel (Fig. 4(b)) arrangements. The mass and energy balances for the control volume, which are the same regardless of the flow arrangement, are:

$$d\dot{m}_w = \dot{m}_a d\omega \quad (1)$$

$$\dot{m}_a dh - \dot{m}_w dh_w - h_w d\dot{m}_w = \dot{m}_a dh - \dot{m}_w c_{p_w} dT_w - c_{p_w} T_w d\dot{m}_w = 0 \quad (2)$$

Heat and mass are transferred from the interface between the water and the air partly as sensible heat, due to temperature difference, and partly as latent heat, due to difference in vapour concentration. The total transfer can be expressed as:

$$d\dot{Q} = d\dot{Q}_s + d\dot{Q}_l \quad (3)$$

The corresponding enthalpy transfer for the mass transfer in Eq. (3) is:

$$d\dot{Q}_l = h_v d\dot{m}_w = h_v h_D (\omega_{s_w} - \omega) dA \quad (4)$$

where $h_v = c_{f_v} + c_{p_v} T_w$. The convective heat transfer is given by:

$$d\dot{Q}_s = h_C (T_w - T) dA \quad (5)$$

In a 1D model of the cooling tower where the available area for heat and mass transfer is the same at any horizontal section through the tower, the transfer area for a section dz can be expressed as $dA = a_V Adz = a_V dV$. Here, a_V is the wetted area divided by the corresponding volume of the tower, A is the corresponding frontal area and V is the cooling tower exchange area volume. According to this, Eqs. (4) and (5) can be rewritten as:

$$d\dot{Q}_l = h_v d\dot{m}_w = h_v h_D a_V (\omega_{s_w} - \omega) dV \quad (6)$$

$$d\dot{Q}_s = h_C a_V (T_w - T) dV \quad (7)$$

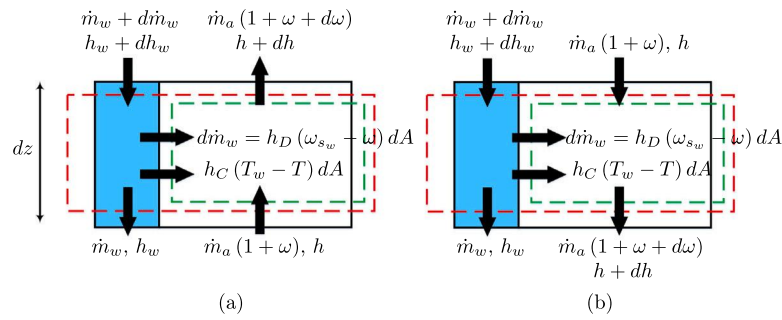


Fig. 4. Control volume in the exchange area of a wet cooling tower. (a) Counterflow and (b) parallel flow arrangements.

Substituting these expressions in Eq. (3):

$$\begin{aligned} d\dot{Q} &= h_C a_V (T_w - T) dV + h_v h_D a_V (\omega_{s_w} - \omega) dV = \\ &= a_V \left[h_C (T_w - T) + h_v h_D (\omega_{s_w} - \omega) \right] dV \end{aligned} \quad (8)$$

The temperature differential in Eq. (8) can be replaced by an enthalpy differential. The enthalpy of saturated air at water temperature is given by Eq. (9), while the enthalpy of the moist air per unit mass of dry air is calculated according to Eq. (10):

$$h_{s_w} = c_{p_a} T_w + \omega_{s_w} h_v = c_{p_a} T_w + \omega h_v + (\omega_{s_w} - \omega) h_v \quad (9)$$

$$h = c_{p_a} T + \omega (c_{f_v} + c_{p_v} T) \quad (10)$$

Hence, the enthalpy difference:

$$\begin{aligned} h_{s_w} - h &= (c_{p_a} + \omega c_{p_v}) (T_w - T) + (\omega_{s_w} - \omega) h_v = \\ &= c_{p_{ma}} (T_w - T) + (\omega_{s_w} - \omega) h_v \end{aligned} \quad (11)$$

where $c_{p_{ma}}$ is the specific heat of the air–water vapour mixture, and is defined as $c_{p_{ma}} = c_{p_a} + \omega c_{p_v}$.

Substituting Eq. (11) into Eqs. (8):

$$\begin{aligned} d\dot{Q} &= a_V \left[h_C \frac{(h_{s_w} - h) - (\omega_{s_w} - \omega) h_v}{c_{p_{ma}}} + h_v h_D (\omega_{s_w} - \omega) \right] dV = \\ &= h_D a_V \left[\frac{h_C}{c_{p_{ma}} h_D} (h_{s_w} - h) + \left(1 - \frac{h_C}{c_{p_{ma}} h_D} \right) h_v (\omega_{s_w} - \omega) \right] \\ &\quad \times dV \end{aligned} \quad (12)$$

where the dimensionless ratio of heat transfer coefficient to mass transfer coefficient is usually regarded as the Lewis factor ($Le = h_C / (c_{p_{ma}} h_D)$). The air enthalpy difference can be obtained upon rearrangement of Eq. (12):

$$\begin{aligned} dh &= \frac{d\dot{Q}}{\dot{m}_a} = \frac{h_D a_V}{\dot{m}_a} \left[Le (h_{s_w} - h) + (1 - Le) h_v (\omega_{s_w} - \omega) \right] dV = \\ &= \frac{h_D a_V}{\dot{m}_a} \left[(h_{s_w} - h) + (Le - 1) \left[(h_{s_w} - h) - (\omega_{s_w} - \omega) h_v \right] \right] dV \end{aligned} \quad (13)$$

Substitute Eqs. (6) and (13) into the energy balance (Eq. (2)):

$$\begin{aligned} \dot{m}_w dh_w &= \dot{m}_a dh - h_w d\dot{m}_w = \\ &= h_D a_V \left[(h_{s_w} - h) + (Le - 1) \left[(h_{s_w} - h) - (\omega_{s_w} - \omega) h_v \right] \right] \\ &\quad \times dV - \\ &\quad - h_w h_D a_V (\omega_{s_w} - \omega) dV = \\ &= h_D a_V \left[(h_{s_w} - h) + (Le - 1) \left[(h_{s_w} - h) - (\omega_{s_w} - \omega) h_v \right] \right] \\ &\quad - (\omega_{s_w} - \omega) h_w \right] dV \end{aligned} \quad (14)$$

Then, combine Eqs. (1) and (2) to find upon rearrangement,

$$\frac{d\omega}{dT_w} = \frac{dh}{T_w dh_w} - \frac{1}{T_w} \frac{\dot{m}_w}{\dot{m}_a} = \frac{\dot{m}_a dh - \dot{m}_w dh_w}{T_w dh_w \dot{m}_a} \quad (15)$$

to finally substitute Eqs. (13) and (14) into Eq. (15) to obtain:

$$\begin{aligned} \frac{d\omega}{dT_w} &= \\ &= \frac{c_{p_w} \frac{\dot{m}_w}{\dot{m}_a} (\omega_{s_w} - \omega)}{\left(h_{s_w} - h \right) + (Le - 1) \left[\left(h_{s_w} - h \right) - (\omega_{s_w} - \omega) h_v \right] - (\omega_{s_w} - \omega) h_w} \end{aligned} \quad (16)$$

Now substitute the expression obtained in Eq. (16) into Eq. (15): (see Eq. (17) in Box I.)

Combining Eqs. (1) and (5), and dividing both sides by \dot{m}_w , it can be found that:

$$\frac{h_D a_V dV}{\dot{m}_w} = \frac{\dot{m}_a}{\dot{m}_w} \frac{d\omega}{\omega_{s_w} - \omega} \quad (18)$$

The left-hand side of Eq. (18) is independent of the thermodynamic conditions in the tower and is determined by the characteristics of the tower design. The dimensionless ratio $h_D a_V V / \dot{m}_w$ is usually known as Merkel number (Eq. (19)), which is the accepted dimensionless coefficient of performance of a wet cooling tower. In the literature, this performance coefficient can also be defined as KaV/L (where $K = h_D$, $a = a_V$ and $L = \dot{m}_w$), Tower Characteristic (TC) or just NTU.

$$Me = \frac{h_D A}{\dot{m}_w} = \frac{h_D a_V V}{\dot{m}_w} \quad (19)$$

According to Eq. (18), the Merkel number can be expressed as:

$$Me = \int \frac{h_D a_V dV}{\dot{m}_w} = \int \frac{\dot{m}_a}{\dot{m}_w} \frac{d\omega}{\omega_{s_w} - \omega} = \int \frac{\dot{m}_a}{\dot{m}_w} \frac{dT_w}{\omega_{s_w} - \omega} \frac{d\omega}{dT_w} \quad (20)$$

Substituting Eq. (16) into Eq. (20),

$$\begin{aligned} \frac{d Me_P}{dT_w} &= \\ &= \frac{c_{p_w}}{\left(h_{s_w} - h \right) + (Le - 1) \left[\left(h_{s_w} - h \right) - (\omega_{s_w} - \omega) h_v \right] - (\omega_{s_w} - \omega) h_w} \end{aligned} \quad (21)$$

The set of coupled ordinary differential equations shown in Eq. (16), (17), and (21) can be solved simultaneously to provide the air humidity, the air enthalpy, the water temperature, the water mass flow rate and the Me profiles in the exchange area of a cooling tower. It should be noted that the equations presented are valid for unsaturated and saturated air. Refer to Kloppers [27] for a detailed derivation of the equations for supersaturated air.

The derivation of the governing equations for heat and mass transfer in the transfer area in the cooling tower was first accomplished by Poppe and Rögner [13]. That is why the set of differential equations presented previously is usually regarded as the Poppe model, and the dimensionless number referred to as Me_P in Eq. (21), is the Merkel number according to the Poppe theory.

$$\frac{dh}{dT_w} = c_{pw} \frac{\dot{m}_w}{\dot{m}_a} \left[1 + \frac{(\omega_{s_w} - \omega) c_{pw} T_w}{(h_{s_w} - h) + (Le - 1) [(h_{s_w} - h) - (\omega_{s_w} - \omega) h_v] - (\omega_{s_w} - \omega) h_w} \right] \quad (17)$$

Box 1.

The system of differential equations can be solved by using the fourth order Runge–Kutta method. Refer to Appendix for the implementation of the Runge–Kutta method to solve the governing equations of the Poppe method.

In this paper, the Poppe method is used for counterflow arrangement (standard variant) and parallel arrangement (less usual variant). Besides, both arrangements are combined in the more rigorous approach proposed in this paper. The main difference in the analysis for both variants (counterflow and parallel), lies in the boundary conditions used (the set of equations remains the same). While in the counterflow arrangement the inlet hot water exchanges heat and mass with the hot humid outlet air, in the case of parallel flow the heat and mass exchange occurs between the inlet hot water and the inlet unsaturated air (see Fig. 4). A more detailed discussion concerning the boundary conditions used in the Poppe model for both flow arrangements can be found in Appendix.

2.2.2. Merkel theory for thermal performance evaluation of wet cooling towers

The Merkel theory [10] for the performance evaluation of cooling towers relies on the following critical assumptions:

- The Lewis factor is equal to 1.
- The air exiting the tower is saturated with water vapour and it is characterised only by its enthalpy.
- The reduction of water flow rate by evaporation is neglected in the energy balance.

Taking into account the third of the above mentioned assumptions, Eq. (2) (energy balance) becomes:

$$\dot{m}_a dh = \dot{m}_w c_{pw} dT_w \quad (22)$$

Substituting Eq. (13) into Eq. (22) and simplifying for Le = 1 (first assumption),

$$\frac{h_D a_V dV}{\dot{m}_w} = c_{pw} \frac{dT_w}{h_{s_w} - h} \quad (23)$$

Integrating:

$$Me_M = \frac{h_D a_V V}{\dot{m}_w} = \int_{T_{w_2}}^{T_{w_1}} \frac{c_{pw}}{h_{s_w} - h} dT_w \quad (24)$$

Here, Me_M is the Merkel number according to the Merkel theory. The Merkel number measures the degree of difficulty of the mass transfer processes taken place in the cooling tower exchange area since the potential for heat and mass transfer at a particular water temperature is the difference between h_{s_w} and h.

The solution of the integral in the right-hand side of Eq. (24) involves thermodynamic properties which are not analytically integrable and needs to be evaluated by numerical integration. The four-point Chebyshev integration technique is recommended by several international standards to determine Me_M. If four intervals are used in conjunction with the trapezoidal rule, the integral, or Merkel number is given by,

$$Me_M = \int_{T_{w_2}}^{T_{w_1}} \frac{c_{pw}}{h_{s_w} - h} dT_w \approx c_{pw} \frac{(T_{w_1} - T_{w_2})}{4} \sum_{j=1}^4 \frac{1}{(h_{s_w} - h)_j} \quad (25)$$

Table 3

Calculation procedure for the counterflow tower characteristic according to the four-point Chebyshev integration technique.

T _w	h _{s_w}	h	(h _{s_w} - h) _j ⁻¹
T _{w₁}		h ₂	
T _{w_A} = T _{w₂} + 0.9 (T _{w₁} - T _{w₂})	h _{s_w} (T _{w_A})	h _A = h ₁ + 0.9 (h ₂ - h ₁)	(h _{s_w} (T _{w_A}) - h _A) ⁻¹
T _{w_B} = T _{w₂} + 0.6 (T _{w₁} - T _{w₂})	h _{s_w} (T _{w_B})	h _B = h ₁ + 0.6 (h ₂ - h ₁)	(h _{s_w} (T _{w_B}) - h _B) ⁻¹
T _{w_C} = T _{w₂} + 0.4 (T _{w₁} - T _{w₂})	h _{s_w} (T _{w_C})	h _C = h ₁ + 0.4 (h ₂ - h ₁)	(h _{s_w} (T _{w_C}) - h _C) ⁻¹
T _{w_D} = T _{w₂} + 0.1 (T _{w₁} - T _{w₂})	h _{s_w} (T _{w_D})	h _D = h ₁ + 0.1 (h ₂ - h ₁)	(h _{s_w} (T _{w_D}) - h _D) ⁻¹
T _{w₂}		h ₁	
			$\sum_{j=1}^4 \frac{1}{(h_{s_w} - h)_j}$

Table 4

Calculation procedure for the parallel tower characteristic according to the four-point Chebyshev integration technique.

T _w	h _{s_w}	h	(h _{s_w} - h) _j ⁻¹
T _{w₁}		h ₁	
T _{w_A} = T _{w₂} + 0.9 (T _{w₁} - T _{w₂})	h _{s_w} (T _{w_A})	h _A = h ₁ + 0.9 (h ₂ - h ₁)	(h _{s_w} (T _{w_A}) - h _A) ⁻¹
T _{w_B} = T _{w₂} + 0.6 (T _{w₁} - T _{w₂})	h _{s_w} (T _{w_B})	h _B = h ₁ + 0.6 (h ₂ - h ₁)	(h _{s_w} (T _{w_B}) - h _B) ⁻¹
T _{w_C} = T _{w₂} + 0.4 (T _{w₁} - T _{w₂})	h _{s_w} (T _{w_C})	h _C = h ₁ + 0.4 (h ₂ - h ₁)	(h _{s_w} (T _{w_C}) - h _C) ⁻¹
T _{w_D} = T _{w₂} + 0.1 (T _{w₁} - T _{w₂})	h _{s_w} (T _{w_D})	h _D = h ₁ + 0.1 (h ₂ - h ₁)	(h _{s_w} (T _{w_D}) - h _D) ⁻¹
T _{w₂}		h ₂	
			$\sum_{j=1}^4 \frac{1}{(h_{s_w} - h)_j}$

The Merkel method is also used in this paper for counterflow and parallel flow arrangements. As previously stated in Section 2.2.1, the main difference between both variants lies in the boundary conditions used. Table 3 shows the calculation procedure for the Merkel number calculated with the Merkel theory for the counterflow arrangement according to the four-point Chebyshev integration technique. As it can be seen, the driving force at the inlet of the exchange area depends on the difference between the inlet hot water (T_{w₁}) and the outlet air (h₂). On the other hand, Table 4 contains the calculation procedure for Merkel number (Merkel theory and Chebyshev integration technique) in parallel flow arrangement. Here, the inlet hot water (T_{w₁}) exchanges heat and mass with the inlet unsaturated air (h₁) at the inlet of the exchange area of the tower.

2.3. Experimental procedure

In this investigation, 5 sets of experiments were carried out to critically evaluate the thermal performance of the cooling tower. According to the literature, the Merkel number depends on the water-to-air mass flow ratio (ṁ_w/ṁ_a). The different levels for the water-to-air mass flow ratio were obtained by changing the air mass flow rate, which was achieved by changing the fan frequency. From the maximum level of 50 Hz to a minimum level of f ≈ 15 Hz. The water mass flow rate was fixed at ṁ_w ≈ 1.3 kg s⁻¹ (f = 50 Hz) in order to avoid modifying the pressure level in the nozzles (it may affect the term a_v). The range for the experimental ṁ_w/ṁ_a values obtained was 0.3–0.8. The thermal load was 30 kW in all tests.

The standards UNE 13741 “Thermal performance acceptance testing of mechanical draught series wet cooling towers” [29], and CTI

Table 5
Averaged values in the experimental test runs.

Test	T_{∞} (°C)	ϕ_{∞} (%)	T_{w_1} (°C)	T_{w_i} (°C)	T_{w_2} (°C)	\dot{m}_a (kg s ⁻¹)	\dot{m}_w (kg s ⁻¹)
1	28.47	71.78	33.39	–	28.13	3.9575	1.3151
2	26.39	76.40	34.40	–	29.22	2.9776	1.3109
3	27.36	62.97	36.02	31.33	30.67	2.5029	1.3088
4	27.23	75.30	40.34	36.74	34.94	2.1145	1.3145
5	30.24	62.23	49.85	49.85	45.47	1.5501	1.3260

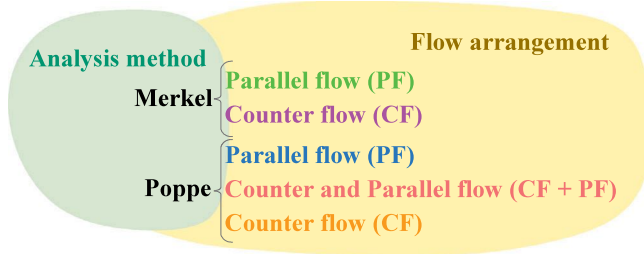


Fig. 5. Methods used in this research for thermal performance evaluation.

“Acceptance Test Code for Water Cooling Towers” [30] were taken as a reference to evaluate the stationary conditions of the tests.

As stated before, the main goal of this work was to conduct a critical evaluation of the heat and mass transfer taken place in the inverted cooling tower. In this sense, the Merkel number has been calculated considering 5 different approaches (listed in Fig. 5).

The two first approaches use the Merkel method considering either parallel arrangement only (as if the cooling would take place only in parallel arrangement) and counterflow arrangement only. They are referred to as Merkel CF and Merkel PF, respectively in Fig. 5. The Poppe approach is also used considering again as if the cooling would take place only in parallel and counterflow arrangement only (Poppe PF and Poppe CF). Besides, since in the novel cooling tower design, heat and mass are transferred partly in counterflow arrangement and partly in parallel arrangement, a more rigorous approach was included in the analysis. This approach takes into account the relative contributions of both flow arrangements and is referred to as Poppe CF + PF in Fig. 5. Fig. 6 schematically depicts the steps taken during the calculation procedure. After a experiment is conducted and all the necessary variables are measured, the Merkel number is calculated according to the 5 approaches previously described. In those approaches where the cooling is considered to take place either in counterflow or parallel arrangement, only the inlet and outlet water temperatures (T_{w_1} , T_{w_2}) are required for the calculation. When the more rigorous approach is used, the intermediate water temperature, T_{w_i} , measured in the water channels is employed alongside with T_{w_1} and T_{w_2} to calculate the cooling taking place in counterflow ($T_{w_1} \rightarrow T_{w_i}$) and parallel arrangement ($T_{w_i} \rightarrow T_{w_2}$).

3. Results and discussion

3.1. Experimental results

Table 5 shows the averaged values of the most relevant ambient and operating conditions during the 5 tests outlined in Section 2.3. It is shown how the water mass flow rate remains constant, while the air mass flow rate decreases from 3.96 to 1.55 kg s⁻¹. Regarding the ambient conditions during the tests, the ambient temperature changed from 24 °C to 30 °C, while the ambient relative humidity from 62% to 76%. The temperature of the water at the different locations (inlet, intermediate and outlet) is also included in Table 5. It is important to mention that there were not always measurements for the intermediate temperature, T_{w_i} , which is measured in the water channels described in Section 2.1 (top right area of the tower depicted in Fig. 3). A visual

Table 6
Merkel number calculated with the different approaches shown in Fig. 5.

Test run	f (Hz)	\dot{m}_w/\dot{m}_a	Merkel		Poppe		
			CF	PF	CF	CF + PF	PF
1	50	0.3323	0.8714	0.9915	0.9055	1.0320	1.0320
2	40	0.4403	0.6145	0.6685	0.6441	0.7017	0.7017
3	30	0.5229	0.4680	0.4971	0.4920	0.4796	0.5233
4	25	0.6217	0.3294	0.3437	0.3487	0.3357	0.3643
5	15	0.8555	0.1135	0.1148	0.1216	0.1230	0.1230

inspection of the water collection channels was carried out during the tests, showing no water being collected in cases where the fan frequency was very high.

The experimental results obtained for the variation of the Merkel number with the water-to-air mass flow ratio, for the 5 approaches studied, are presented in Table 6.

These results are presented in Fig. 7. The $Me - \dot{m}_w/\dot{m}_a$ relationship follows the expected trend: Me decreases potentially with \dot{m}_w/\dot{m}_a (linear trend on log-log scale). This involves that the effect of \dot{m}_w/\dot{m}_a on Me becomes less pronounced as \dot{m}_w/\dot{m}_a increases. This behaviour is attributed to the decrease in the fraction of water that evaporates per unit of inlet water with increasing \dot{m}_w/\dot{m}_a values. The situation corresponding to the minimum \dot{m}_w/\dot{m}_a can be interpreted as the maximum air flow rate for a given water flow rate to be cooled. This results in the maximum driving force and, therefore, maximum Merkel number. As \dot{m}_a decreases progressively, the driving force decreases for a given \dot{m}_w , and Me decreases accordingly. The experimental uncertainty has been calculated according to the ISO Guide [31], with the type B evaluation for standard uncertainty and a coverage factor of $k = 2$ (level of confidence of 95%) for the expanded uncertainty. The sensor specifications were taken as a reference for the calculations (Table 2). Averaged values of 3.53%, and 11.73% were obtained for \dot{m}_w/\dot{m}_a and Me , respectively. It should be mentioned that the above values were calculated for the Merkel theory and counterflow arrangement. No significant variations for the uncertainty levels were observed for the rest of methods of analysis or the flow arrangements considered in this paper.

The sequence in terms of decreasing Merkel number is Poppe method in parallel arrangement, Poppe method in combined counterflow and parallel arrangement, Merkel method in parallel arrangement, Poppe counterflow, and Merkel counterflow.

The Merkel method for wet cooling tower performance evaluation tends to underestimate the performance characteristics of the tower. The Merkel number, determined by the Poppe theory for the trickle fill employed in the inverted cooling tower, is 5.13% higher than the Merkel number determined by the Merkel method. This difference is roughly constant regardless of the flow arrangement considered (parallel or counterflow) and changes slightly with the water-to-air mass flow ratio tested (3.84% with $\dot{m}_w/\dot{m}_a = 0.33$ and 6.64% with $\dot{m}_w/\dot{m}_a = 0.86$).

Concerning the influence of the flow arrangement on the thermal performance analysis, the Merkel number calculated for the parallel arrangement is higher than the one obtained for the counterflow arrangement. This statement is valid for the Merkel number calculated with both, Poppe and Merkel theories. On average, the difference is 6.32%, with a maximum of 12% for some water-to-air mass flow ratios. This fact can be explained as a higher transfer coefficient being

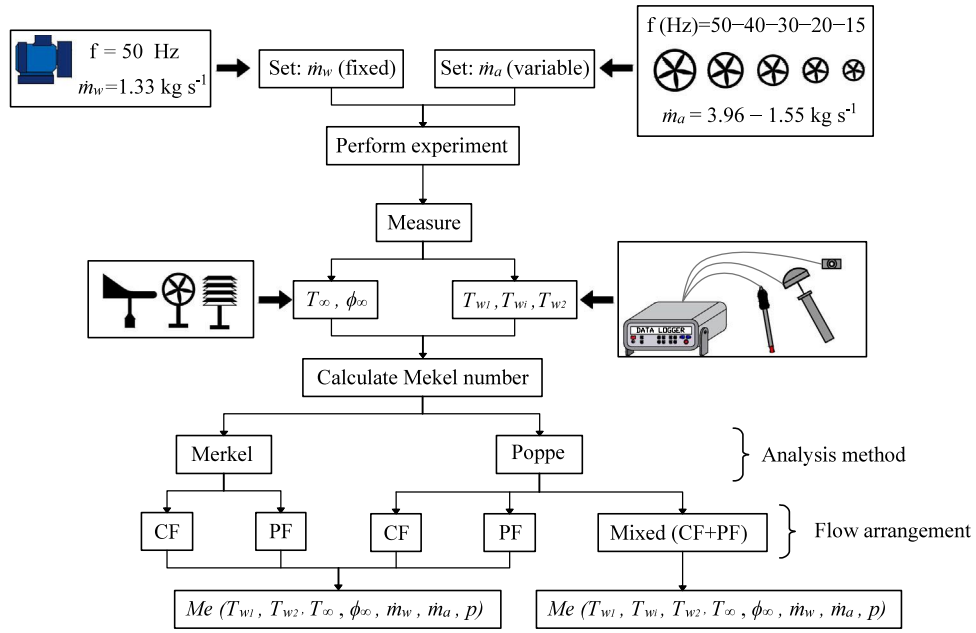


Fig. 6. Merkel number calculation procedure flowchart.

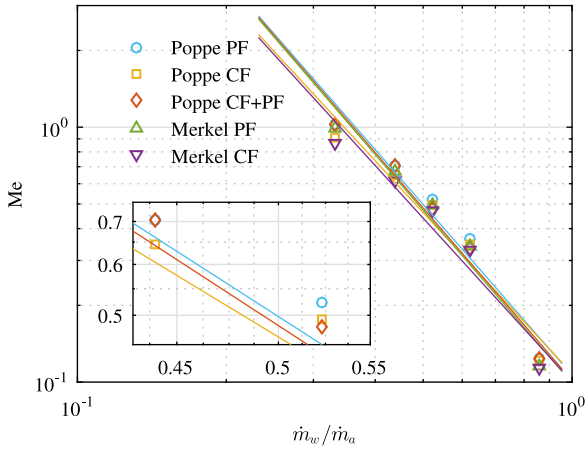


Fig. 7. Experimental results for the Me number as a function of \dot{m}_w/\dot{m}_a .

required to achieve the same cooling for parallel arrangement compared to counterflow arrangement. If the results obtained with the parallel arrangement and the Poppe method are compared with those obtained with the rigorous approach proposed in this research, they are slightly higher (average difference $\sim 3.24\%$). When compared to the counterflow arrangement, the results obtained with the proposed model are 5.57% higher on average. These results follow the logical sequence $Me_{PF} > Me_{CF+PF} > Me_{CF}$, since the rigorous approach includes both arrangements and the results are closer to a totally parallel behaviour.

Table 7 shows the results predicted by the rigorous method proposed in this paper. It presents the Merkel number calculated for each flow arrangement, the total Merkel number ($Me_{CF+PF} = Me_{CF} + Me_{PF}$) and the contribution of the parallel and counterflow arrangements as a fraction of the total cooling (Me_{PF} / Me_{CF+PF} and Me_{CF} / Me_{CF+PF}).

As it can be seen, the cooling occurs mostly in parallel arrangement for high fan frequencies ($f > 40$ Hz), as well as for low frequencies ($f \approx 15$ Hz). The cooling is mixed (counterflow and parallel) for intermediate frequency levels.

For those cases where the fan frequency is very high, the highest height reached by the water (where the arrangement of the flows

Table 7

Values of the Merkel number and the contribution of each flow arrangement, in the experimental thermal tests carried out.

Test run	f (Hz)	\dot{m}_w/\dot{m}_a	Me_{CF}	Me_{PF}	Me_{CF+PF}	$\frac{Me_{CF}}{Me_{CF+PF}}$	$\frac{Me_{PF}}{Me_{CF+PF}}$
1	50	0.3323	0.0000	1.0320	1.0320	0.00	1.00
2	40	0.4403	0.0000	0.7017	0.7017	0.00	1.00
3	30	0.5229	0.4070	0.0726	0.4796	0.85	0.15
4	25	0.6217	0.2048	0.1309	0.3357	0.61	0.39
5	15	0.8555	0.0000	0.1230	0.1230	0.00	1.00

changes) is very close to the location where the nozzles are placed. Therefore, it can be said that the counterflow cooling in this case is practically zero and therefore, all the cooling occurs in parallel. As the frequency of the fan decreases, water is collected in the channels and it is possible to identify the amount of counterflow and parallel cooling. Finally, for the lowest fan frequency level tested, the water reaches the channels without modifying its temperature, probably because the short time required to reach the top height. Therefore, for these cases the counterflow cooling is zero and all cooling occurs in parallel. Fig. 8 graphically attempts to explain this behaviour.

Table 7 includes the ratios of the cooling occurring in parallel and counterflow to the total cooling, in terms of the Merkel number. It can be seen that the Merkel number calculated in counterflow arrangement initially increases when the air mass flow rate decreases (increasing the water droplets travelling distance). Subsequently, the Merkel number calculated in counterflow arrangement begins to decrease while the water-to-air mass flow ratio increases. This is justified because for very high water-to-air mass flow ratios the air flow rate is low and, therefore, the cooling capacity decreases (term h_D).

3.2. Correlation and validation

As stated in Section 2.3, the transfer coefficient of the tower (Merkel number) depends on the water-to-air mass flow ratio. In this sense, the calculated Me has been correlated as a function of \dot{m}_w/\dot{m}_a (Eq. (26)) as suggested by [28,32,33], among others.

$$Me = c \left(\frac{\dot{m}_w}{\dot{m}_a} \right)^{-n} \quad (26)$$

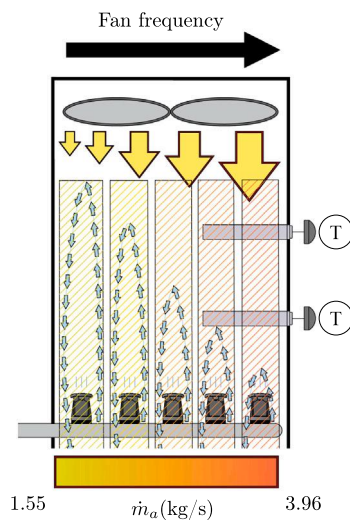


Fig. 8. Channel location and flow arrangement.

Table 8
Constants c and n for the Poppe and Merkel theories and the different flow arrangements.

Method	c	n
Poppe PF	0.1066	2.2227
Poppe CF	0.1081	2.0977
Poppe CF + PF	0.1014	2.2479
Merkel PF	0.0991	2.2532
Merkel CF	0.1005	2.1292

Table 9
Maximum and averaged difference between calculated and measured outlet water temperatures.

Method	Max dif. (%)	Averaged dif. (%)
Poppe PF	1.94	1.36
Poppe CF	2.11	1.60
Poppe CF + PF	2.08	1.31
Merkel PF	1.97	1.36
Merkel CF	2.13	1.59

The solid lines in Fig. 7 correspond to the transfer characteristic of the cooling tower, described by Eq. (26). Constants c and n in the equation can be found in Table 8 for the 5 approaches analysed.

This information regarding the transfer coefficient is commonly used in the cooling tower analysis to predict the water outlet temperature. The results of the comparison between calculated and measured outlet water temperatures, for the 5 approaches analysed are remarkably confident (Table 9). For the proposed rigorous approach, the maximum and averaged differences between experimental and predicted results are 0.74 °C and 0.44 °C, respectively. This translates into a maximum percentage difference of 2.08% (~ 1.31% on average). No significant differences were observed in the results regardless of the model used or the arrangement considered. Fig. 9 shows the calculated and experimental outlet water temperatures for the 5 approaches analysed in this paper.

Notwithstanding the observed differences between the Merkel numbers calculated with the Poppe and Merkel methods, the subsequent application of the Merkel method employing the smaller value for the Merkel number obtained during cooling tower tests, will predict nearly the same cooling tower water outlet temperature as obtained by the Poppe method.

As the Poppe method provides the air profiles (humidity ratio and enthalpy) in the transfer region of the cooling tower both, the evolution of the air properties and the outlet temperature, can be predicted.

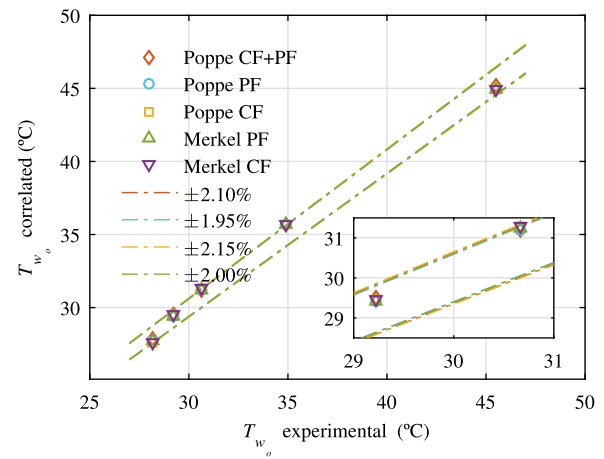


Fig. 9. Comparison between experimental and predicted cooling tower outlet water temperatures.

The evolution of the air and water properties in the psychrometric chart is displayed in Fig. 10 for three different experimental tests. The solid lines overlapping the saturation curve depict the evolution of the water, since the driving force in the cooling process depends on the difference between the enthalpy of the saturated air evaluated at the water temperature and the air enthalpy.

It can be observed how the air is heated up and increases its moisture contents while evolving to the outlet water temperature. In the case corresponding to the largest fan frequency level tested ($f = 50$ Hz, blue series in Fig. 10), the temperature evolution is shorter due to the smaller contact time between air and water due to the large air velocity. Besides, the temperature difference near the outlet of the cooling tower is $T > T_w$. This implies that the sensible heat transfer is from the air to the water while the latent heat transfer is from the water to the air. The net enthalpy transfer is still in the direction of the air. As a result, in this area both, the air and the water, are cooled. In the case corresponding to $f = 25$ Hz, the air evolution in both arrangements is presented in different colours (yellow and green). It can be seen how both predictions provide the same air temperature at the location of the nozzles.

The maximum difference between calculated and measured outlet air temperatures for the Poppe theory using the rigorous approach combining both flow arrangements is 1.33 °C (~4.30%), and the average is 0.58 °C (1.95%). Those values highlight the goodness of the proposed approach of analysis. Similar average differences, though slightly worse, are observed in counterflow and parallel arrangement by the Poppe method to those obtained by the proposed method. Note that the Merkel approach does not predict the air outlet temperature.

In the light of the results obtained, it can be said that choosing a particular method of analysis when evaluating the performance characteristics of the tower is important, because this method must subsequently be employed in the analytical approach to predict cooling tower performance. In this sense, if only the water outlet temperature is of relevance, any of the approaches described in this paper can be used, as they predict practically identical water outlet temperatures. However, in the case of the inverted tower, using the Poppe method of analysis including both of the transfer arrangements is suggested. Not only it provides the best predictions for the outlet water and air temperatures but it is a good approximation of the complex underlying physics of the problem and the state of the outlet air is accurately determined.

4. Conclusions

In this study, a critical evaluation of the heat and mass transfer processes taken place in a mechanical forced draft, counterflow-parallel

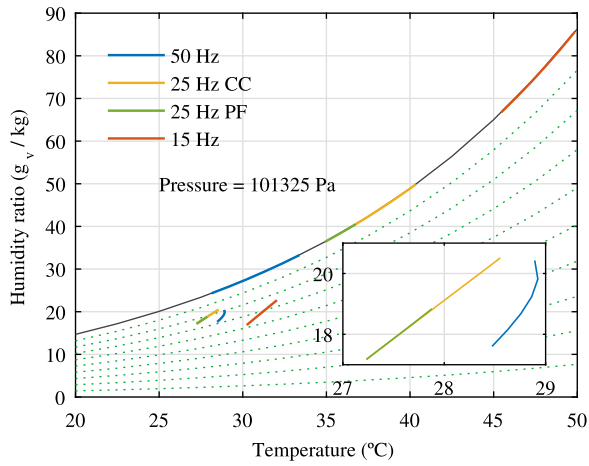


Fig. 10. Evolution of the properties of water and air in a psychrometric chart.

flow, wet cooling tower (known as inverted cooling tower) has been investigated. The results obtained during the research can be summarised as follows:

It has been assessed, by experimental observation, that the tower cools the water in both, parallel and counterflow, flow arrangements. Hence, a rigorous approach that uses the Poppe theory and combines both flow arrangements is proposed to evaluate the thermal performance of the novel cooling tower prototype.

The amount of cooling taking place in the counterflow arrangement increases and then decreases with decreasing fan frequency. This is because for high fan frequency levels the drag force rapidly overcomes the momentum of the water droplets when they are sprayed and for low fan frequency levels the contact time between the air and the water in counterflow arrangement is small.

In the light of the results obtained in this research, the proposed approach of analysis is the best way to evaluate the thermal characteristic of the cooling tower prototype. It provides remarkable predictions for the outlet water and air temperatures. On average, 0.44 °C difference for the water prediction and 0.74 °C difference for the air prediction are observed.

The Merkel and Poppe methods of analysis for thermal performance prediction, report differences ranging from 3.84% to 6.64% ($Me_p > Me_M$). The particular method of analysis when evaluating the performance characteristics of a certain fill material must subsequently be employed in the analytical approach to predict cooling tower performance. If only the water outlet temperature is of relevance, the Merkel approach can be used, as it predicts practically identical water outlet temperatures than the Poppe approach.

The influence of the flow arrangement on the thermal performance prediction has also been investigated. A higher Merkel number is obtained for the parallel arrangement compared to counterflow to achieve the same cooling. Differences from 1.12% to 12.19% are observed for the range of tested water-to-air mass flow ratios. This fact is justified by the higher transfer coefficient required to achieve the same cooling for parallel arrangement compared to counterflow arrangement.

CRedit authorship contribution statement

P. Navarro: Investigation, Formal analysis, Writing – original draft, Writing – review & editing. **J. Ruiz:** Methodology, Formal analysis, Writing – original draft, Writing – review & editing, Funding acquisition. **M. Hernández:** Conceptualization, Investigation, Formal analysis. **A.S. Kaiser:** Conceptualization, Writing – review & editing, Supervision, Funding acquisition. **M. Lucas:** Conceptualization, Writing – review & editing, Supervision, Funding acquisition.

Declaration of competing interest

The authors declare that they have no known competing financial interests or personal relationships that could have appeared to influence the work reported in this paper.

Acknowledgements

The authors acknowledge the financial support received from the Spanish Government and from the Government of Valencia (Generalitat Valenciana), Spain, through projects ENE2017-83729-C3-3-R (MINECO/AEI/FEDER, UE) and BEST/2019/051 (Subvenciones para estancias de personal investigador doctor en centros de investigación radicados fuera de la Comunitat Valenciana). The authors wish to acknowledge the collaboration in the experimental work of Julio Parra Saura for his amazing work as a lab technician. This paper was presented and published in the proceedings of the 15th International Conference on Heat Transfer, Fluid Mechanics and Thermodynamics (HEFAT2021), Online, 26–28 July 2021.

Appendix. Solving the system of differential equations by means of the fourth order runge–kutta method

The fourth order Runge–Kutta method is used to solve the system of differential equations shown in Eq. (16), (17), and (21), which can be written as:

$$\frac{d\omega}{dT_w} = f_1(\omega, h, T_w) \tag{A.1}$$

$$\frac{dh}{dT_w} = f_2(\omega, h, T_w) \tag{A.2}$$

$$\frac{dMe_p}{dT_w} = f_3(\omega, h, T_w) \tag{A.3}$$

The calculation procedure is detailed below:

- The transfer area is divided into levels with the same water temperature difference across each interval, Eq. (A.4).
- Levels (imaginary horizontal planes at the top and bottom of the transfer area and between two intervals) are also specified (see Fig. A.11).
- Initial values of the variables T_w , h and ω are required on a particular level, say level (n). This point is of high relevance when analysing different flow arrangements. For a counterflow arrangement, the initial values for the variables at level 0 are $T_{w(0)} = T_{w_2}$, $h_{(0)} = h_1$ and $\omega_{(0)} = \omega_1$. In the parallel arrangement however, $T_{w(0)} = T_{w_2}$, $h_{(0)} = h_2$ and $\omega_{(0)} = \omega_2$.
- The values of the variables can then be determined at level ($n+1$) with the aid of the Eqs. (A.5)–(A.7). Here, j , k and l are calculated using Eqs. (A.8)–(A.19).

$$\Delta T_w = \frac{(T_{w_1} - T_{w_2})}{N} \tag{A.4}$$

$$w_{(n+1)} = w_{(n)} + \frac{j_{(n+1,1)} + 2j_{(n+1,2)} + 2j_{(n+1,3)} + j_{(n+1,4)}}{6} \tag{A.5}$$

$$h_{(n+1)} = h_{(n)} + \frac{k_{(n+1,1)} + 2k_{(n+1,2)} + 2k_{(n+1,3)} + k_{(n+1,4)}}{6} \tag{A.6}$$

$$Me_{p(n+1)} = Me_{p(n)} + \frac{l_{(n+1,1)} + 2l_{(n+1,2)} + 2l_{(n+1,3)} + l_{(n+1,4)}}{6} \tag{A.7}$$

$$j_{(n+1,1)} = \Delta T_w \cdot f_1(T_{w(n)}, h_{(n)}, w_{(n)}) \tag{A.8}$$

$$k_{(n+1,1)} = \Delta T_w \cdot f_2(T_{w(n)}, h_{(n)}, w_{(n)}) \tag{A.9}$$

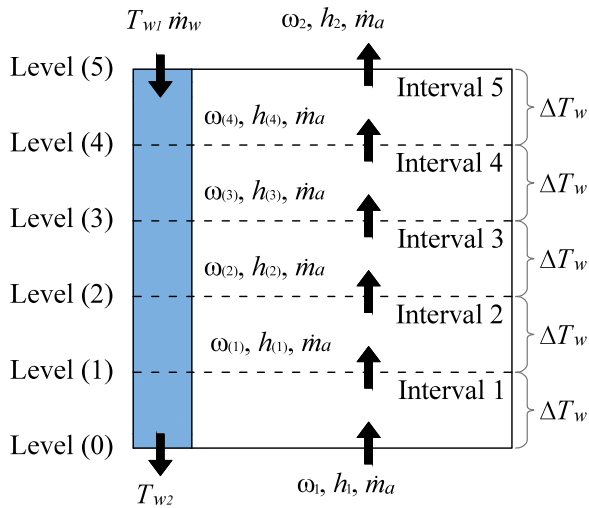


Fig. A.11. Counterflow cooling tower exchange area divided into five intervals.

$$l_{(n+1,1)} = \Delta T_w \cdot f_3 \cdot (T_{w(n)}, h_{(n)}, w_{(n)}) \quad (\text{A.10})$$

$$j_{(n+1,2)} = \Delta T_w \cdot f_1 \cdot \left(T_{w(n)} + \frac{\Delta T_w}{2}, h_{(n)} + \frac{k_{(n+1,1)}}{2}, w_{(n)} + \frac{j_{(n+1,1)}}{2} \right) \quad (\text{A.11})$$

$$k_{(n+1,2)} = \Delta T_w \cdot f_2 \cdot \left(T_{w(n)} + \frac{\Delta T_w}{2}, h_{(n)} + \frac{k_{(n+1,1)}}{2}, w_{(n)} + \frac{j_{(n+1,1)}}{2} \right) \quad (\text{A.12})$$

$$l_{(n+1,2)} = \Delta T_w \cdot f_3 \cdot \left(T_{w(n)} + \frac{\Delta T_w}{2}, h_{(n)} + \frac{k_{(n+1,1)}}{2}, w_{(n)} + \frac{j_{(n+1,1)}}{2} \right) \quad (\text{A.13})$$

$$j_{(n+1,3)} = \Delta T_w \cdot f_1 \cdot \left(T_{w(n)} + \frac{\Delta T_w}{2}, h_{(n)} + \frac{k_{(n+1,2)}}{2}, w_{(n)} + \frac{j_{(n+1,2)}}{2} \right) \quad (\text{A.14})$$

$$k_{(n+1,3)} = \Delta T_w \cdot f_2 \cdot \left(T_{w(n)} + \frac{\Delta T_w}{2}, h_{(n)} + \frac{k_{(n+1,2)}}{2}, w_{(n)} + \frac{j_{(n+1,2)}}{2} \right) \quad (\text{A.15})$$

$$l_{(n+1,3)} = \Delta T_w \cdot f_3 \cdot \left(T_{w(n)} + \frac{\Delta T_w}{2}, h_{(n)} + \frac{k_{(n+1,2)}}{2}, w_{(n)} + \frac{j_{(n+1,2)}}{2} \right) \quad (\text{A.16})$$

$$j_{(n+1,4)} = \Delta T_w \cdot f \cdot (T_{w(n)} + \Delta T_w, h_{(n)} + k_{(n+1,3)}, w_{(n)} + j_{(n+1,3)}) \quad (\text{A.17})$$

$$k_{(n+1,4)} = \Delta T_w \cdot g \cdot (T_{w(n)} + \Delta T_w, h_{(n)} + k_{(n+1,3)}, w_{(n)} + j_{(n+1,3)}) \quad (\text{A.18})$$

$$l_{(n+1,4)} = \Delta T_w \cdot h \cdot (T_{w(n)} + \Delta T_w, h_{(n)} + k_{(n+1,3)}, w_{(n)} + j_{(n+1,3)}) \quad (\text{A.19})$$

The four variables in the Runge–Kutta method are T_w , ω , h and Me_p from the left-hand side of Eqs. (16), (17), and (21). For this reason Eqs. (A.1)–(A.3) are functions of only T_w , ω , and h . Most of the other variables are functions of these variables. Eqs. (A.1)–(A.3) are not functions of Me_p because dMe_p/dT_w is a function of $d\omega/dT_w$ as can be seen from Eq. (20). Thus, Eqs. (16) and (17) can be solved without Eq. (21).

References

- [1] S.R. Hanna, J. Pell, Cooling tower environment—1974, *Environ. Pollut.* 10 (1976) 237, (1970).
- [2] J.J. Talbot, A review of potential biological impacts of cooling tower salt drift, *Atmos. Environ.* 13 (1979) 395–405, (1967).
- [3] D.C. McCune, Effects of airborne saline particles on vegetation in relation to variables of exposure and other factors, *Environ. Pollut.* 74 (1991) 176–203.
- [4] EPA, AP-42. Compilation of Air Pollutant Emission Factors, Environmental Protection Agency. Office of Air Quality Planning and Standards, United States, 1995.
- [5] V.A. Mouchtouri, G. Goutziana, J. Kremastinou, C. Hadjichristodoulou, Legionella species colonization in cooling towers: Risk factors and assessment of control measures, *Am. J. Infect. Control* 38 (2010) 50–55.
- [6] J. Ruiz, P. Navarro, M. Hernández, M. Lucas, A.S. Kaiser, Thermal performance and emissions analysis of a new cooling tower prototype, *Appl. Therm. Eng.* (2022) 118065.
- [7] BOE, RD 865/2003. Hygienic-Sanitary Criteria for the Prevention and Control of Legionellosis, Spanish Ministry of Health and Consume, 2003.
- [8] AS, AS-4180.1. Drift Loss from Cooling Towers; Laboratory Measurement. Part 1: Chloride Balance Method, Standards Australia, 1994.
- [9] J. Ruiz, P. Navarro, M. Hernández, M. Lucas, A.S. Kaiser, Experimental study on the thermal performance of a new prototype of cooling tower, in: *Proceedings of the 15th International Conference on Heat Transfer, Fluid Mechanics and Thermodynamics*, 2021.
- [10] F. Merkel, Verdunstungskühlung, *VDI Z. Dtsch. Ing.* (1925) 123–128.
- [11] C. Bourillot, Hypotheses of calculation of the water flow rate evaporated in a wet cooling tower, 1983.
- [12] H. Jaber, R.L. Webb, Design of cooling towers by the effectiveness-NTU method, *J. Heat Transfer* 111 (1989) 837–843.
- [13] M. Poppe, H. Rögner, Berechnung von Rückkühlwerken, *VDI Wärmeatlas* (1991) Mi 1.
- [14] T. Ke, X. Huang, X. Ling, Numerical and experimental analysis on air/water direct contact heat and mass transfer in the humidifier, *Appl. Therm. Eng.* 156 (2019) 310–323.
- [15] B. Mishra, A. Srivastava, L. Yadav, Performance analysis of cooling tower using desiccant, *Heat Mass Transf.* 56 (2019) 1153–1169.
- [16] G. Zengin, A. Onat, Experimental and theoretical analysis of mechanical draft counterflow wet cooling towers, *Sci. Technol. Built Environ.* 27 (2020) 14–27.
- [17] X. Huang, Y. Li, T. Ke, X. Ling, W. Liu, Thermal investigation and performance analysis of a novel evaporation system based on a humidification-dehumidification process, *Energy Convers. Manage.* 147 (2017) 108–119.
- [18] Y. Zhou, X. Zhu, X. Ding, Theoretical investigation on thermal performance of new structure closed wet cooling tower, *Heat Transf. Eng.* 39 (2018) 460–472.
- [19] O.T. Bamimore, S. Enibe, P.A. Adedeji, Parametric effects on the performance of an industrial cooling tower, *J. Therm. Sci.* 7 (2021) 904–917.
- [20] A.C.C. Tomás, S.D.O. Araujo, M.D. Paes, A.R.M. Primo, J.A.P. Da Costa, A.A.V. Ochoa, Experimental analysis of the performance of new alternative materials for cooling tower fill, *Appl. Therm. Eng.* 144 (2018) 444–456.
- [21] M.M. Keshtkar, Performance analysis of a counter flow wet cooling tower and selection of optimum operative condition by MCDM-TOPSIS method, *Appl. Therm. Eng.* 114 (2017) 776–784.
- [22] Y. Li, X. Huang, H. Peng, X. Ling, S. Tu, Simulation and optimization of humidification-dehumidification evaporation system, *Energy* 145 (2018) 128–140.
- [23] K. Singh, R. Das, Simultaneous optimization of performance parameters and energy consumption in induced draft cooling towers, *Chem. Eng. Res. Des.* 123 (2017) 1–13.
- [24] J. Liao, X. Xie, H. Nemer, D.E. Claridge, C.H. Culp, A simplified methodology to optimize the cooling tower approach temperature control schedule in a cooling system, *Energy Convers. Manage.* 199 (2019) 111950.
- [25] M.H. Sharqawy, I. Al-Shalawi, M.A. Antar, S.M. Zubair, Experimental investigation of packed-bed cross-flow humidifier, *Appl. Therm. Eng.* 117 (2017) 584–590.
- [26] A. Ayoub, B. Gjorgiev, G. Sansavini, Cooling towers performance in a changing climate: Techno-economic modeling and design optimization, *Energy* 160 (2018) 1133–1143.
- [27] J.C. Kloppers, A Critical Evaluation and Refinement of the Performance Prediction of Wet-Cooling Towers (Ph.D. thesis), University of Stellenbosch, South Africa, 2003.
- [28] J.C. Kloppers, D.G. Kröger, A critical investigation into the heat and mass transfer analysis of counterflow wet-cooling towers, *Int. J. Heat Mass Transfer* 48 (2005) 765–777.
- [29] UNE, Thermal Performance Acceptance Testing of Mechanical Draught Series Wet Cooling Towers, UNE, 2004.

- [30] CTI, Code Tower, Standard Specifications. Acceptance Test Code for Water Cooling Towers, Cooling Technology Institute, 2000.
- [31] J.C. for Guides in Metrology (JCGM), Evaluation of Measurement Data. Guide to the Expression of Uncertainty in Measurement, 2008.
- [32] Ashrae, HVAC systems and equipment, in: Cooling Towers, 2004 (Chapter 36).
- [33] M. Lucas, J. Ruiz, P.J. Martínez, A.S. Kaiser, A. Viedma, B. Zamora, Experimental study on the performance of a mechanical cooling tower fitted with different types of water distribution systems and drift eliminators, *Appl. Therm. Eng.* 50 (2013) 282–292.